Title

Drumming motor sequence training induces myelin remodelling in Huntington's disease: a longitudinal diffusion MRI and quantitative magnetization transfer study

Running title

Myelin remodelling in Huntington's disease

Key words

Huntington's disease, drumming training, white matter, myelin, diffusion MRI

Authors

Chiara Casella[1*], Jose Bourbon-Teles[1*], Sonya Bells[2], Elizabeth Coulthard[3], Greg Parker[1], Anne Rosser[4,6], Derek Jones[1,5], Claudia Metzler-Baddeley[1]

*These authors share first authorship

Affiliations

[1] Cardiff University Brain Research Imaging Centre (CUBRIC), School of Psychology, Cardiff University, Maindy Road, Cardiff, CF 24 4HQ, UK [2] The Hospital for Sick Children, Neurosciences and Mental Health, Toronto, M5G 1X8, Canada; [3] Clinical Neurosciences, University of Bristol, Bristol, BS10 5NB, UK, [4] School of Biosciences,

Cardiff University, Museum Avenue, Cardiff, CF10 3AX, UK. [5] Mary MacKillop Institute for Health Research, Australian Catholic University, Melbourne, Victoria 3065, Australia.[6] Department of Neurology and Psychological Medicine, Hayden Ellis Building, Maindy Rd, CF24 4HQ

Corresponding author

Chiara Casella, CUBRIC, Maindy Road, Cardiff CF24 4 HQ, CasellaC@cardiff.ac.uk.

Declarations

Ethics approval and consent to participate

The study was approved by the local National Health Service (NHS) Research Ethics Committee (Wales REC 1 13/WA/0326) and all participants provided written informed consent.

Availability of data and materials

The datasets analysed during the current study are available from the corresponding author on reasonable request.

Competing interests

The authors declare that they have no competing interests.

Authors' contributions

CMB designed the study, obtained the funding which made the study possible; helped with the set-up and completion of the study; contributed to the interpretation of results. JBT was responsible for data collection, helped with MRI data processing, carried out tractography of the tracts investigated, and helped with scoring the drumming assessment. SB and GP helped with MRI data processing. CC processed some of the data, performed statistical analysis on the data, interpreted results and wrote the paper. GDP helped with the processing pipeline of the diffusion data. DKJ helped with the interpretation of results. AR and EC helped with patients' recruitment and undertook UHDRS assessments.

Funding & Acknowledgements

The present research was funded by a Wellcome Trust Institutional Strategic Support Fund Award (ref:506408) to CMB, AR, and DKJ and a Wellcome Trust PhD studentship to CC (ref: 204005/Z/16/Z); DKJ is supported by a New Investigator Award from the Wellcome Trust (096646/Z/11/Z).

We would like to thank Candace Ferman and Louise Gethin for collating the patients' clinical details and Jilu Mole for assistance with data analysis.

63 **List of abbreviations**

64 MRI: magnetic resonance imaging

65 DTI: diffusion tensor imaging

66 DT MRI: diffusion tensor magnetic resonance imaging

67 FA: fractional anisotropy

68 FR: restricted fraction

69 RD: radial diffusivity

70 MPF: macromolecular proton fraction

71 qMT: quantitative magnetization transfer

72 CHARMED: Composite Hindered and Restricted Model of Diffusion

73 WM: white matter

74 GM: grey matter

75 HD: Huntington's disease

76 CC: corpus callosum

77 SMA: supplementary motor area

78 UHDRS: Unified Huntington's disease rating scale

79 PCA: principal component analysis

80 TMS: total motor score

FAS: functional assessment score

MT: magnetization transfer

EPI: echo planar imaging

fODF: fiber orientation density function

ROI: region of interest

SD: standard deviation

ANOVA: analysis of variance

CI: confidence intervals

FDR: false discovery rate

TBSS: tract-based spatial statistics

FWE: family-wise error

Abstract

Background: Huntington's disease (HD) is a neurodegenerative disorder leading to debilitating cognitive and motor symptoms. Impaired myelination may contribute to HD pathogenesis. We assessed baseline differences in apparent white matter (WM) myelination between HD patients and controls, and tested whether drumming training stimulates myelin remodelling in HD. We also examined whether microstructural changes were related to changes in motor and cognitive function. **Methods**: Participants undertook two months of drumming exercises. Different aspects of

working memory and executive function were assessed before and after the training. For comparability with previous studies, we assessed training-related changes in diffusion tensor magnetic resonance imaging (DT-MRI)-based metrics of fractional anisotropy (FA) and radial diffusivity (RD). Moving beyond DT-MRI, we also tested changes in the restricted diffusion signal fraction (Fr) from the composite hindered and restricted model of diffusion (CHARMED) and in the macromolecular proton fraction (MPF) from quantitative magnetization transfer (qMT). We predicted the biggest training effects in MPF, because of its greater sensitivity to myelin, compared to diffusion measures. Changes were studied in WM pathways linking the putamen and the supplementary motor area (SMA-Putamen), and within three segments of the corpus callosum (CCI, CCII, CCIII). Tracts were reconstructed using deterministic tractography. Baseline MPF differences between patients and controls were also assessed with tract-based spatial statistics (TBSS), to inspect HD-associated changes in apparent myelination. **Results:** A reduction in baseline MPF was present in the mid section of the CC in HD group compared to controls. No significant training-associated changes were detected in FA, RD or Fr. However, after the drumming intervention, we detected increases in MPF in HD patients relative to healthy controls in the CCII, CCIII, and the right SMA-putamen. Furthermore patients improved their drumming and their executive function performance relative to controls increased after training**.** These behavioural changes did not correlate with the microstructural changes, suggesting that these processes follow different time courses. **Conclusions:** Drumming training improves motor and executive performance in HD and is associated with increases in apparent WM myelin. Tailored behavioural stimulation may lead to neural benefits in early HD that could be exploited for delaying disease progression.

125 **Background**

126 Huntington's disease (HD) is a genetic, neurodegenerative disease caused by
127 an expansion of the CAG repeat within the coding region of the *huntingtin* gene,
128 leading to debilitating cognitive and motor symptoms. Although HD pathology is tightly
129 associated with degeneration of striatal grey matter (GM) (Weaver et al., 2009), WM
130 changes at the macro- and micro-structural level have recently been suggested to play
131 an important role in this disease (Bardile et al., 2018; Bartzokis et al., 2007; Beglinger
132 et al., 2007; Ciarmiello et al., 2006; Gregory et al., 2018; Paulsen et al., 2008; Reading
133 et al., 2005; Rosas et al., 2018; Wang & Yang, 2019), and can be detected even in
134 pre-symptomatic individuals, 15 years or more prior to the onset of motor symptoms
135 (Aylward et al., 2011; Ciarmiello et al., 2006; Tabrizi et al., 2009).

136 An increasing body of research suggests that WM alterations in HD are due to
137 changes in myelin-associated biological processes at the cellular and molecular level
138 (Gómez-Tortosa et al., 2001; Huang et al., 2015; Jin et al., 2015; Myers et al., 1991;
139 Simmons et al., 2007; Teo et al., 2016). Myelin is a multi-layered membrane sheath
140 wrapping axons and is produced by oligodendrocytes. Axon myelination is vital during
141 brain development and critical for healthy brain function, as it plays a fundamental role
142 in the efficiency and speed of action potential propagation (Martenson, 1992).

143 The 'Demyelination Hypothesis' of HD (Bartzokis et al., 2007) suggests that a
144 toxic effect of mutant huntingtin leads to myelin breakdown in HD. This could be due
145 to several factors: dysregulation of the temporal profile of myelination during the
146 postnatal period (Jin et al., 2015) or dysfunction in oligodendrocytes, leading to
147 impaired repair of demyelinated axons (Huang et al., 2015); alternatively, as
148 oligodendrocytes are the major iron-containing cells of the CNS, homeostatic

149 increases in these cells in the attempt to re-myelinate axons might lead to significant
150 increases in ferritin iron content, leading to toxicity and contributing to impairments in
151 myelination (Bourbon-Teles et al., 2017).

152 Currently, no disease-modifying treatment exists for HD. However,
153 environmental stimulation and behavioural interventions may have the potential to
154 delay disease onset (van Dellen et al., 2000; Yhnell et al., 2016). Interestingly, myelin
155 plasticity is thought to support the learning of new motor skills (McKenzie et al., 2014;
156 Sampaio-Baptista et al., 2013). Accordingly, recent evidence from animal and human
157 studies suggests that plastic changes in myelination may be implicated in early
158 adaptation and longer-term consolidation and improvement in motor tasks (Costa,
159 Cohen, & Nicolelis, 2004; Shmuelof & Krakauer, 2011; Steele, Bailey, Zatorre, &
160 Penhune, 2013; Yin et al., 2009).

161 In the present study, we assessed whether two months of drumming training
162 could trigger WM microstructure changes, and potentially myelin remodelling, in
163 individuals with HD. Based on reports of greater training-associated changes in
164 structural MRI metrics in patient populations than in healthy subjects (Caeyenberghs
165 et al., 2018), we hypothesised that these changes would be present to a higher degree
166 in patients than in healthy subjects.

167 The present drumming intervention was designed to exercise cognitive and
168 motor functions including sequence and reversal learning, response speed and multi-
169 tasking (Metzler-Baddeley et al., 2014), all of which rely on healthy functioning of
170 cortico-basal ganglia loops and are known to be impaired in HD (Papoutsi et al., 2014).
171 In brief, the training involves practising drumming patterns in ascending order of

difficulty over a period of two months and was previously found to induce WM microstructural changes in HD (Metzler-Baddeley et al. 2014).

Previous studies investigating training-associated WM plasticity in the human brain (Giacosa, Karpati, Foster, Metzler-Baddeley et al. 2014; Penhune, & Hyde, 2016; Scholz, Klein, Behrens, & Johansen-Berg, 2009) have predominantly employed indices from diffusion tensor magnetic resonance imaging (DT-MRI) (Pierpaoli & Basser, 1996) such as fractional anisotropy (FA) and radial diffusivity (RD). However, DT-MRI measures are not specific to WM microstructural properties and can be modulated by various factors, including, but not limited to, fibre complexity and organisation, as well as axon morphology and myelination (De Santis et al., 2014; Wheeler-Kingshott & Cercignani, 2009). It is therefore difficult to interpret changes in DTI indices in terms of changes in any biological properties of white matter.

Moving beyond DT-MRI, the present study explored changes in the macromolecular proton fraction (MPF) from quantitative magnetization transfer (qMT) (Sled, 2018) and the restricted diffusion signal fraction (Fr) from the composite hindered and restricted model of diffusion (CHARMED) (Assaf & Basser, 2005), as well as FA and RD from DT-MRI (Pierpaoli & Basser, 1996), for comparability with previous training studies (Lövdén et al., 2010; Scholz et al., 2009; Zatorre, Fields, & Johansen-Berg, 2012).

MPF identifies the ratio of the number of bound macromolecular protons to the total water protons, and has been proposed as a proxy MRI marker of myelin (Serres et al., 2009). Accordingly, this measure has been shown to reflect demyelination in shiverer animals (Ou, Sun, Liang, Song, & Gochberg, 2009; Samsonov et al., 2012), to be sensitive to de-myelination processes in multiple sclerosis patients (Levesque et

al., 2010) and to reflect myelin content of WM in post-mortem studies of multiple sclerosis brains (Schmierer et al., 2007). Fr, on the other hand, represents the fraction of signal that is restricted, which is presumed to come predominantly from within axons, and therefore provides a proxy measure of axonal density (Barazany, Basser, & Assaf, 2009).

Based on evidence suggesting an effect of motor learning on myelin plasticity (Lakhani et al., 2016;), we were especially interested in assessing training-associated changes in MPF, because of its tight association with WM myelin content (Levesque et al., 2010; Ou et al., 2009; Schmierer et al., 2007; Serres et al., 2009). Therefore, we expected changes following training to be more marked in MPF, as compared to the other non-myelin sensitive metrics assessed in this study.

Additionally, while the plastic regulation of myelination by neural activity and experience has gained increased recognition and has been demonstrated in recent studies (Hofstetter, Tavor, Moryosef, & Assaf, 2013; Lakhani et al., 2016; Sampaio-Baptista et al., 2013), the role of myelin remodelling in shaping behavioural changes remains elusive. Therefore, we also investigated the relationship between training-associated changes in MRI measures and changes in drumming performance and in different aspects of cognitive/executive function. The latter was assessed with standard neuropsychological paper and pencil tests before and after the training as described in Metzler-Baddeley et al. (2014).

Because of the sensitivity of MPF to myelin content in WM, we were also interested in using this measure to investigate baseline myelin differences between HD patients and controls across the brain. Previous evidence has shown widespread decreases in MPF in early-stage HD patients as compared to healthy controls

(Bourbon-Teles et al., 2019). Therefore, tract-based spatial statistics (TBSS) (Smith et al., 2006) was used to investigate differences in MPF between HD subjects and controls before training, across the whole brain, in an unbiased way.

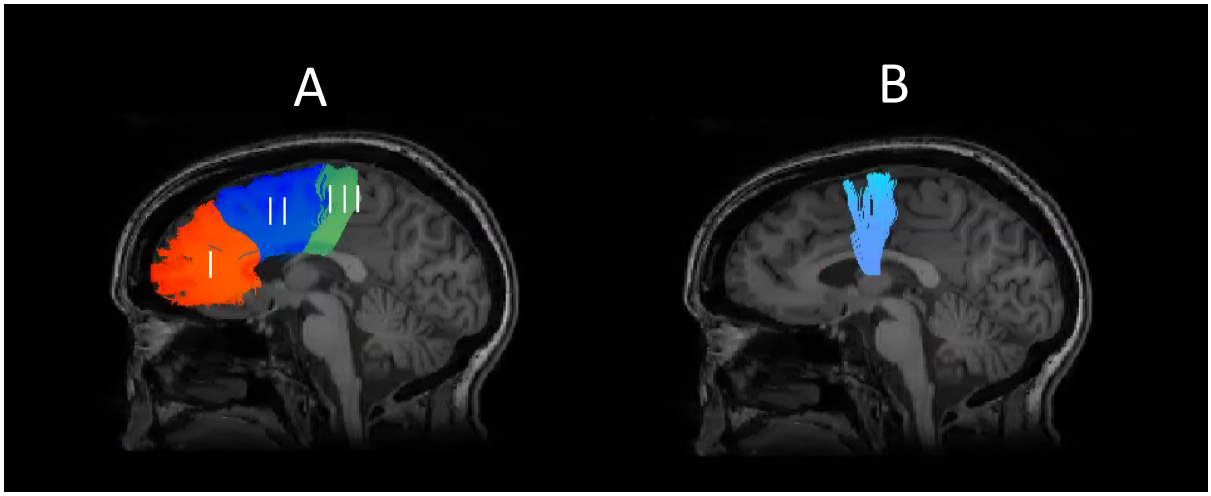

Figure 1. White matter pathway regions of interest. *Sagittal views of the reconstructed WM pathways displayed on a T_1-weighted image for one control participant. (A) Segments I, II, and III of the CC (Hofer and Frahm, 2006), (B) SMA-putamen pathway. Fibre directions are colour coded with green indicating directions along the coronal, blue along the axial and red along the sagittal plane (Pajevic & Pierpaoli, 1999).*

Materials and Methods

Participants

The study was approved by the local National Health Service (NHS) Research Ethics Committee (Wales REC 1 13/WA/0326) and all participants provided written informed

consent. All participants were drumming novices and none had taken part in our previously-reported pilot study (Metzler-Baddeley et al., 2014). Fifteen HD patients, most of which were at early disease stages (see Table 1), as assessed by their performance in the United Huntington's Disease Rating Scale (UHDRS), were recruited from HD clinics in Cardiff and Bristol. Genetic testing confirmed the presence of the mutant huntingtin allele. Table 1 summarizes the patients' demographic and some background clinical characteristics, i.e. their CAG repeat length, their UHDRS Total Motor Score (TMS) and UHDRS Functional Assessment Score (FAS), and information about their medication.

Thirteen age, sex, and education matched healthy controls were recruited from the School of Psychology community panel at Cardiff University and from patients' spouses, carers or family members. Participants were eligible to take part in the study if they had no history of head injury, stroke or cerebral haemorrhages. Control participants were excluded if they had a history of neurological or psychiatric conditions and patients if they had a history of any other neurological conditions. All patients had to be on stable medication for a minimum of four weeks prior to the study and during the study. Participants also had to be eligible for MRI scanning i.e. to not present contraindications such as pacemakers, metal clips, stents or significant chorea which would have prevented them from lying still in the scanner. Two patients were not MRI compatible, four patients withdrew during the study and one patient's MRI data had to be excluded due to excessive motion. In total, MRI data could be analysed for eight of the patients. Out of the thirteen control participants, one participant had to be excluded due to an incidental MRI finding and two participants dropped out of the study. One participant turned out not eligible for MRI. Thus, in total MRI data from nine

controls were available for analyses. Table 2 summarizes information about demographic variables and performance in the Montreal Cognitive Assessment (MoCA) (Nasreddine et al., 2005) and in the revised National Adult Reading Test (NART-R) (Nelson, 1991) for those patients and controls whose MRI data were included in the analyses. Both groups did not differ significantly in age or the MoCA score. However, controls were on average slightly older and performed better on the MoCA. Controls also had a significantly higher NART-IQ than patients.

Table 1. *Demographics and background clinical information of the patients for which the MRI data could be analysed.*

Patient	Age	Sex	Length of CAG repeats	TMS	FAS	Medications
HD1	22	M	51	17	23	Citalopram 30 mg
HD2	47	M	46	69	18	Sertraline50 mg
HD3	62	F	41	4	25	Novate ointments, Naproxen
HD4	50	M	40	0	25	Nil
HD5	68	F	43	40	17	Mirtazapine 30 mg
HD6	58	M	43	0	25	Atorvastatin 20 mg
HD7	30	F	42	0	25	Nil
HD8	51	M	43	20	23	Co-codamol 500 mg, Brufen 400 mg
Mean	48.5		43.625	18.75	22.625	
SD	15.62		3.46	24.65	3.29	

Abbreviations: CAG = cytosine-adenine-guanine, F = Female, M = Male, TMS = Total Motor Score out of 124 (the higher the scores the more impaired the performance). FAS = Functional Assessment Score out of 25 (the higher the scores the better the performance). HD = Huntington's disease, SD = Standard Deviation.

Table 2. *Demographics and general cognitive profile of patients and controls. Both groups were matched for age, sex and years of education but the patient group performed less well than the control group in the MoCA.*

Mean (SD)	Patients (n = 8)	Controls (n = 9)	t-statistic (p-value)
Age	48.5 (15.62)	52.6 (14.56)	t(15) = 0.554 (0.59)
NART-IQ	106.3 (13.13)	121.22 (4.32)	t(15) = 3.212 (0.006)
MoCa	23 (5.6)	27.67 (1)	t(15) = 2.463 (0.26)

Abbreviations: MoCA = Montreal Cognitive Assessment score out of 30; NART-IQ = verbal IQ estimate based on the National Adult Reading Test.

Training intervention: Drumming-based rhythm exercises

The same rhythm exercise and drumming training as described in Metzler-Baddeley et al. (2014) was applied. Patients and controls were provided with twenty-two 15 min training sessions on CDs, a pair of bongo drums and a drumming diary and could practice the drumming exercise at home. Each training session introduced a drumming pattern, and trainees had to drum along with the instructor and to reproduce as accurately as possible the timing and temporal speed of each bongo beat. The complexity and speed of the drumming patterns increased gradually over the sessions. Participants were asked to train for 15 min per day, 5 times per week, for 2 months (40 sessions in total), and to record each training session in the diary. Compliance was also monitored with regular weekly phone calls. Whenever possible, carers and/or spouses were also involved to support and encourage participants with the training. Participants were instructed to repeat each session at least twice but could progress through the training at their own pace and repeat sessions more often

300 if they felt it necessary. Control participants started with Session 3 since the first two
301 exercises were designed for patients.

302

303 ***Drumming assessment***

304 Any progress in drumming ability was assessed by digitally recording
305 participants' drumming performance for three patterns of ascending levels of difficulty
306 (easy, medium and hard), which were not part of the training sessions, at baseline and
307 after the training. Each recording was judged by an independent rater, blind to group
308 and time, according to an adopted version of the Trinity College London marking
309 criteria for percussion (2016) (www.trinitycollege.com). This comprised categories of
310 rhythm, synchronization with backing track, accuracy, hand control, use of available
311 percussion, and general confidence and style. Drumming performance was assessed
312 for each category on a five point rating scale from poor (1) to excellent (5) with a
313 maximal possible score of 30.

314

315 **Cognitive assessments**

316 Different aspects of cognition and executive function were assessed with
317 standard neuropsychological paper and pencil tests before and after the training as
318 described in Metzler-Baddeley et al. (2014). Parallel versions of all tests matched for
319 difficulty were used and counterbalanced across participants and time of
320 assessments. Multi-tasking was assessed with a dual task requiring simultaneous box
321 crossing and digit sequences repetition (Baddeley, 1996). Attention switching was
322 assessed with the trails test (VT) requiring the verbal generation of letter and digit

323 sequences in alternate order relative to a baseline condition of generating letter or digit
324 sequences only (Baddeley, 1996). Distractor suppression was tested with the Stroop
325 task involving the naming of incongruent ink colours of colour words (Trenerry et al.,
326 1989). Verbal and category fluency were tested using the letter cues “F”, “A”, “S” and
327 “M”, “C”, “R” as well as the categories of “animals” and “boys’ names” and
328 “supermarket items” and “girls’ names” respectively (Baldo, Shimamura, Delis,
329 Kramer, & Kaplan, 2001). In total, we assessed 7 outcome variables, and percentage
330 change scores in performance were computed for each of these variables (Table 3).

331

332 ***MRI data acquisition***

333 MRI data were acquired on a 3 Tesla General Electric HDx MRI system (GE Medical
334 Systems, Milwaukee) using an eight channel receive-only head RF coil at the Cardiff
335 University Brain Research Imaging Centre (CUBRIC). The MRI protocol comprised
336 the following images sequences: high-resolution T_1-weighted, diffusion-weighted and
337 quantitative magnetization transfer. The acquisition of the T_1-weighted anatomical
338 image (FSPGR) was based on the following parameters: 256 x 256 acquisition matrix,
339 TR = 7.8 ms, TE = 2.9 ms, flip angle = 20, 172 slices, 1mm slice thickness, FOV =
340 23cm. Diffusion data were acquired employing a spin-echo echo- planar sequence
341 with diffusion encoded along 60 isotropically-distributed orientations according to an
342 optimized gradient vector scheme (Jones et al., 1999) and six non-diffusion weighted
343 scans (96 x 96 acquisition matrix, TR/TE = 87ms, b-value = 1200 s/mm^2, 60 slices,
344 2.4 mm slice thickness, spatial resolution 1.8 x 1.8 x 2.4 mm). Diffusion data
345 acquisition was peripherally gated to the cardiac cycle with a total acquisition time of
346 ~30 min depending on the heart rate.

Table 3. *Cognitive outcome variables assessed in this study. Tests were carried out before and after the training, and a percentage change score was computed for each variable.*

Outcome variable	Cognitive Test	Brief Description
Number of correct digits recalled under single task condition	Dual task requiring simultaneous box crossing and digit sequences repetition (Baddeley, 1996)	Correct number of recalled digits in a standard digit span test.
Number of correct digits recalled under dual task conditions	Dual task requiring simultaneous box crossing and digit sequences repetition (Baddeley, 1996)	Correct number of recalled digits in the dual condition, which combines box-crossing and digit span.
Total number of boxes identified under dual task condition	Dual task requiring simultaneous box crossing and digit sequences repetition (Baddeley, 1996)	Number of boxes identified in the dual condition, which combines box-crossing and digit span.
Stroop interference score	Stroop test (Trenerry et al., 1989)	Calculated by subtracting the number of errors from the total number of items presented in the test.
Trail test switching	Trials test (Baddeley, 1996)	Performance accuracy: reflects the ability of moving flexibly from one set of rules to another in response to changing task requirements.
Verbal fluency	Verbal and category fluency test (Delis et al., 2001)	Number of generated words starting with the following letters: “F”, “A”, “S” and “M”, “C”, “R”
Category fluency	Verbal and category fluency test (Delis et al., 2001)	Number of generated words belonging to the following categories: “animals” and “boys’ names” and “supermarket items” and “girls’ names”.

In addition, Fr maps were acquired using the CHARMED protocol (Assaf and Basser, 2005) (slice thickness: 2.4mm, FE: 126 ms, TR: 17,000 ms; 45 gradient orientations distributed on 8 shells; maximum b-value: 8700s/mm^2; FOV: 230 mm x 230 mm, acquisition matrix: 96 x 96).

To obtain MPF maps, an optimized 3D MT-weighted fast spoiled gradient recalled-echo (SPGR) sequence (Cercignani and Alexander, 2006) was used with the following parameters: TR/TE = 25.82/2.18 ms; Gaussian MT pulses, duration t = 14.6

358 ms; acquisition matrix = 96x96x60; BW=±244Hz. The following off-resonance
359 irradiation frequencies (Θ) and their corresponding saturation pulse amplitude (ΔSAT)
360 for the 11 Magnetization transfer (MT) weighted images were optimized using Cramer-
361 Rao lower bound optimization (Cercignani & Alexander, 2006): D = [1000 Hz, 1000
362 Hz, 12062 Hz, 47185 Hz, 56363 Hz, 2751 Hz, 1000 Hz, 1000 Hz, 2768 Hz, 2791 Hz,
363 2887 Hz] and their corresponding qSAT = [332°, 333°, 628°, 628°, 332°, 628°, 628°,
364 628°, 628°, 628°, 628°]. Longitudinal relaxation rate of the system was estimated using
365 3D SPGRs (TR = 6.85 ms, TE = 1.2 ms, FOV and resolution is the same as the MT
366 sequence) with three different flip angles (theta = 1 °, 7 °, 3 °). B_0 maps consisted of
367 two 3D spoiled, gradient recalled acquisitions (SPGR), which were collected with
368 different echo-times (TE = 9ms and 7ms respectively; TR= 20ms; matrix=128x128;
369 FOV= 220 mm; slice thickness 3mm) (Jezzard and Balaban, 1995).
370

371 ***MRI data processing***

372 The diffusion-weighted data were corrected for distortions induced by the
373 diffusion-weighted gradients, artifacts due to head motion and due to echo planar
374 imaging (EPI) induced geometrical distortions by registering each image volume to the
375 T_1-weighted anatomical images (Irfanoglu, Walker, Sarlls, Marenco, & Pierpaoli,
376 2012), with appropriate reorientation of the encoding vectors (Alexander Leemans &
377 Jones, 2009), all done in ExploreDTI (Version 4.8.3) (Leemans, Jeurissen, Sijbers, &
378 Jones, 2009). A two-compartment model was then fitted to derive maps of FA and RD
379 in each voxel (Metzler-Baddeley, O'Sullivan, Bells, Pasternak, & Jones, 2012).
380 CHARMED data were corrected for motion and distortion artefacts according to the
381 extrapolation method of Ben-Amitay, Jones, and Assaf (2012). The number of distinct

382 fiber populations (1, 2, or 3) in each voxel was obtained using a model selection
383 approach (De Santis et al., 2014) and Fr was calculated per voxel with an in-house
384 software (De Santis et al., 2014) coded in MATLAB (The MathWorks, Natick, MA)

385 MT-weighted SPGR volumes for each participant were co-registered to the MT-
386 volume with the most contrast using an affine (12 degrees of freedom, mutual
387 information) registration to correct for inter-scan motion using Elastix (Klein, Staring,
388 Murphy, Viergever, & Pluim, 2010). The 11 MT-weighted SPGR images and T_1 map
389 were modelled by the two pool Ramani's pulsed MT approximation (Henkelman et al.,
390 1993; Ramani et al., 2002), which included corrections for amplitude of radio-
391 frequency (B_0 and B_1) field inhomogeneities. This approximation provided MPF maps,
392 which were nonlinearly warped to the T1-weighted imaging using the MT-volume with
393 the most contrast as a reference using Elastix (normalized mutual information cost
394 function) (add REF).

395

396 ***Deterministic Tractography***

397 Training-related changes in FA, RD, Fr, and MPF were quantified using a
398 tractography approach to localize measurements to specific WM pathways, i.e. those
399 interconnecting the putamen and the supplementary motor area bilaterally (SMA-
400 Putamen), and within three segments of the corpus callosum (CCI, CCII and CCIII)
401 (Hofer & Frahm, 2006) (Figure 1).

402 The SMA has efferent and afferent projections to the primary motor cortex and
403 is involved in movement execution, and previous evidence suggests that symptomatic
404 HD patients present altered DT-MRI metrics in the putamen-motor tracts (Poudel et

al., 2014). The anterior and anterior-mid sections of the corpus callosum contain fibres connecting the motor, premotor and supplementary motor areas in each hemisphere (Hofer & Frahm, 2006). Previous work has demonstrated a thinning of the corpus callosum in post-mortem HD brains (Vonsattel & Difiglia, 1998), altered diffusion tensor metrics in the corpus callosum of both pre-symptomatic and symptomatic HD patients (Rosas et al., 2010; Phillips et al., 2013), and a correlation between these metrics and performance on tests assessing motor function (Dumas et al., 2012).

Whole brain tractography was performed for each participant in their native space using the damped Richardson-Lucy algorithm (Dell'acqua et al., 2010), which allows the recovery of multiple fiber orientations within each voxel including those affected by partial volume. The tracking algorithm estimated peaks in the fiber orientation density function (fODF) by selecting seed points at the vertices of a 2 × 2 × 2 mm grid superimposed over the image and propagated in 0.5-mm steps along these axes re-estimating the fODF peaks at each new location (Jeurissen, Leemans, Jones, Tournier, & Sijbers, 2011). Tracks were terminated if the fODF threshold fell below 0.05 or the direction of pathways changed through an angle greater than 45° between successive 0.5 mm steps. This procedure was then repeated by tracking in the opposite direction from the initial seed-points.

Three-dimensional tractograms of the WM tracts of interest were extracted from the whole-brain tractograms by applying way-point of interest gates (Catani et al., 2002). ROIs were drawn manually by one operator (JBT) blind to the identity of each dataset on color-coded fiber orientation maps in native space guided by the following anatomical landmark protocols (Figure 2).

429 Corpus callosum

430 The reconstructions of the segments of the CC followed the protocol by Hofer
431 and Frahm (Hofer & Frahm, 2006) and are illustrated in Figure 2A. Firstly, the midline
432 of the CC located between the most anterior point of the genu and the most posterior
433 point of the splenium was identified and the CC was divided into an anterior and a
434 posterior half. CCI, the most anterior portion of the CC that maintains prefrontal
435 connections between both hemispheres, was reconstructed by placing a sagittal
436 SEED ROI of about 1/6 of the anterior half of the CC around the genu. CCII, the portion
437 that maintains connections between premotor and supplementary motor areas of both
438 hemispheres, was reconstructed by placing a sagittal way-point of interest gate
439 between the posterior edge of Segment I and the midline of the corpus CC. Segment
440 III, the portion that maintains connections between primary motor cortices of both
441 hemispheres, was reconstructed by placing a sagittal gate immediately after the
442 midline covering about 1/3 of the posterior half of the CC. Segment reconstructions
443 were visually inspected and if necessary gates were placed to exclude any streamlines
444 that were not consistent with the known anatomy of the CC.

445 SMA-putamen pathway

446 One axial way-point gate was placed around the putamen and one axial gate
447 around the supplementary motor cortex (Leh, Ptito, Chakravarty, & Strafella, 2007)
448 (Figure 2B). A way-point gate to exclude brain stem fibers was placed inferior to the
449 putamen.

450

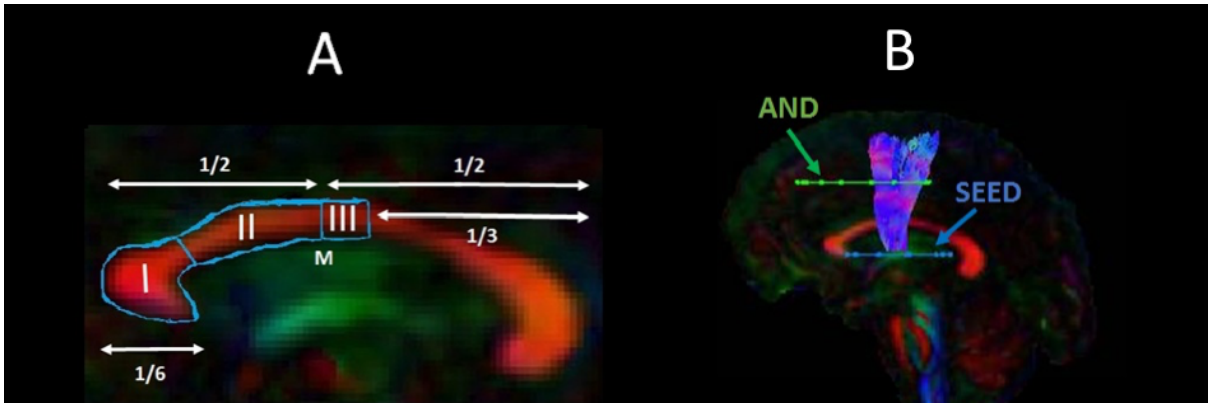

Figure 2. Sagittal views of the tractography protocols. *(A) Segments I, II and III of the corpus callosum (B) SMA - putamen pathway. Booleian logic OR waypoint regions of interest gates are illustrated in blue; AND gates in green. M = Midline.*

Statistical analyses

Statistical analyses were carried out in R Statistical Software (Foundation for Statistical Computing, Vienna, Austria).

<u>Assessment of training effects on drumming performance</u>

Improvements in drumming performance were analysed with repeated measure analysis of variance (ANOVA) testing for the effects of group (HD, controls), time of assessment (before and after the training) and group by time interaction effects. Significant effects were further explored with *post-hoc* paired and independent t-tests. The reliability of the *post-hoc* analyses was assessed with bootstrap analysis based on 1000 samples and the 95% confidence interval (CI) of the mean difference is provided for each significant comparison.

468 Assessment of group differences in the effect of training on cognitive performance

469 Performance measures in executive function tasks have been shown to share
470 underlying cognitive structures (Testa, Bennett, & Ponsford, 2012). Therefore, PCA
471 was employed to reduce the complexity of the cognitive data and hence the problem
472 of multiple comparisons as well as to increase experimental power. PCAs were run
473 on change scores for all participants across both groups. Because of the relatively
474 small sample size, we first confirmed with the Kaiser-Meyer-Olkin (KMO) test that our
475 data was suited for PCA. Subsequently, we followed guidelines to limit the number of
476 extracted components (Preacher & MacCallum, 2002; Winter, Dodou, & Wieringa,
477 2009), as follows: first, we employed the Kaiser criterion of including all components
478 with an eigenvalue greater than 1; second, we inspected the Cattell scree plot (Cattell,
479 1966) to identify the minimal number of components that accounted for most variability
480 in the data; third, we assessed each component's interpretability. A PCA procedure
481 with orthogonal Varimax rotation of the component matrix was used. Loadings that
482 exceeded a value of 0.5 were considered as significant.

483 Next, we assessed group differences in the component scores with permutation
484 analyses, to understand whether the training had differentially affected HD patients as
485 compared to controls. Significant group differences were tested using 5,000
486 permutations. Permutation testing relies only on minimal assumptions and can
487 therefore be applied when the assumptions of a parametric approach are untenable
488 such as in the case of small sample sizes. Multiple comparison correction was based
489 on a 5% false discovery rate (FDR) using the Benjamini-Hochberg procedure
490 (Benjamini & Hochberg, 1995).

491

492 Training effects on WM microstructure

493 Median measures of FA, RD, Fr and MPF were derived for each of the
494 reconstructed tracts in ExploreDTI. A percentage change score in these measures
495 between baseline and post-training was calculated in each tract (CCI, CCII, CCIII, left
496 and right SMA-Putamen).

497 Previous research has shown that variation in the microstructural properties of
498 WM may represent a global effect, rather than being specific to individual tracts, and
499 that WM measures are highly correlated across WM areas (Lövdén et al., 2010; Penke
500 et al., 2010; Wahl et al., 2010). Therefore, we inspected the correlation matrices for
501 each of the measures investigated and found that MPF values were highly correlated
502 across tracts, whereas this was not true for the other metrics (Figure 3).

503 Hence, as for the cognitive data, percentage change scores in MPF across the
504 different tracts were transformed with PCA in order to extract meaningful anatomical
505 properties. Because of the relatively small sample size for PCA, we followed guidelines
506 to limit the number of extracted components (Preacher & MacCallum, 2002; Winter,
507 Dodou, & Wieringa, 2009), as described above for the PCA of cognitive change
508 scores.

509 PC scores for each participant were used as dependent variables in a
510 permutation-based analysis using 5,000 permutations to assess group differences in
511 training associated changes in MPF. Finally, as post-hoc exploration, we tested
512 whether we could detect between-groups differences in MPF changes in the individual
513 tracts using 5000 permutations.

514

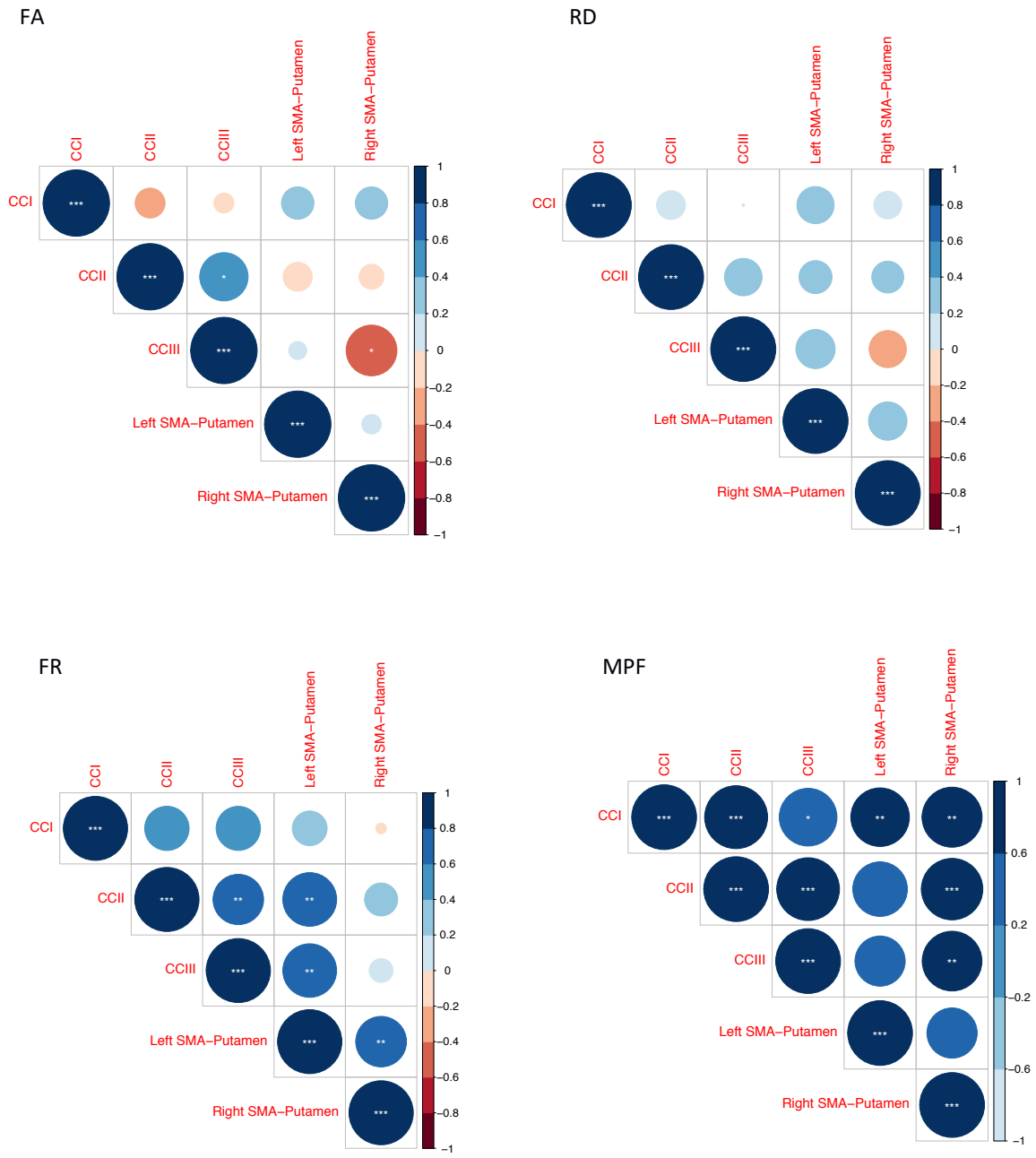

Figure 3. Correlation matrices for the MRI metrics investigated across the different WM pathways. *Colour intensity and the size of the circles are proportional to the strength of the correlation. * p < 0.05, ** p < 0.01, *** p < 0.001.* MPF *values were highly correlated across tracts, whereas this was not true for the other metrics*

522 Training-associated changes in FA, Fr and RD were investigated with
523 permutation analyses separately for each tract. Significant group differences in these
524 measures were tested using 5,000 permutations. Multiple comparison correction was
525 based on a 5% FDR using the Benjamini-Hochberg procedure (Benjamini & Hochberg,
526 1995).

527 TBSS (Smith et al., 2006) was carried out to investigate baseline differences in
528 MPF voxelwise between HD subjects and healthy controls. First, a mean FA image
529 was created and thinned to generate a mean FA skeleton, thought to represent the
530 centres of all WM tracts common to the sample investigated. Subsequently, all
531 subjects' warped MPF data were merged into a 4D file, and this was projected onto
532 the original mean FA skeleton (using the original FA data to find the projection vectors),
533 resulting in MPF 4D projected data.

534 To produce significance maps, a voxel-wise analysis was performed on the
535 MPF projected 4D data for all voxels with FA ≥ 0.20 to exclude peripheral tracts where
536 significant inter-subject variability exists. Inference based on permutations (5,000
537 permutations) and threshold-free-cluster-enhancement were used. The significance
538 level was set at $p < 0.05$ and corrected by multiple comparisons (family-wise error,
539 FWE). Maps of significance were generated to identify differences in areas of MPF
540 between patients with HD and controls.

541 <u>Relationship between changes in MRI measures and changes in drumming and</u>
542 <u>cognitive performance</u>

543 We computed percentage change scores for the drumming performance, in the
544 same way cognitive change scores were calculated. Scores were computed for the

easy test pattern in patients and for the medium test pattern in controls, as these were the training patterns that showed a significant improvement.

Spearman correlation coefficients were calculated between drumming and cognitive performance, and microstructural components that showed significant group differences, to assess whether microstructural changes were related to any drumming and/or cognitive benefits of the training.

Results

Training effects on drumming performance

The repeated measure ANOVA of the ratings of drumming performance for the easy and medium test pattern showed significant group [easy: $F(1,17) = 19.6$, $p \leq 0.001$; medium: $F(1,17) = 13.1$, $p = 0.002$] and time effects [easy: $F(1,17) = 10.95$, $p \leq 0.004$; medium: $F(1,17) = 13.4$, $p = 0.002$] but no interaction effects (easy: $p = 0.8$; medium: $p=0.3$). For the hard test pattern there was only a significant group effect [$F(1,17) = 9.95$, $p = 0.006$] but no time ($p = 0.1$) or interaction effects ($p = 0.4$), Figure 4 summarises the average drumming performance per group and time point. Overall patients' drumming performance was poorer than controls. Patients improved their drumming performance significantly for the easy pattern [$t(10) = 2.7$, $p = 0.02$; 95% CI: 1.5 – 7.8] and controls for the medium pattern [$t(7) = 3.8$, $p = 0.01$; 95% CI: 2.8 – 8.5].

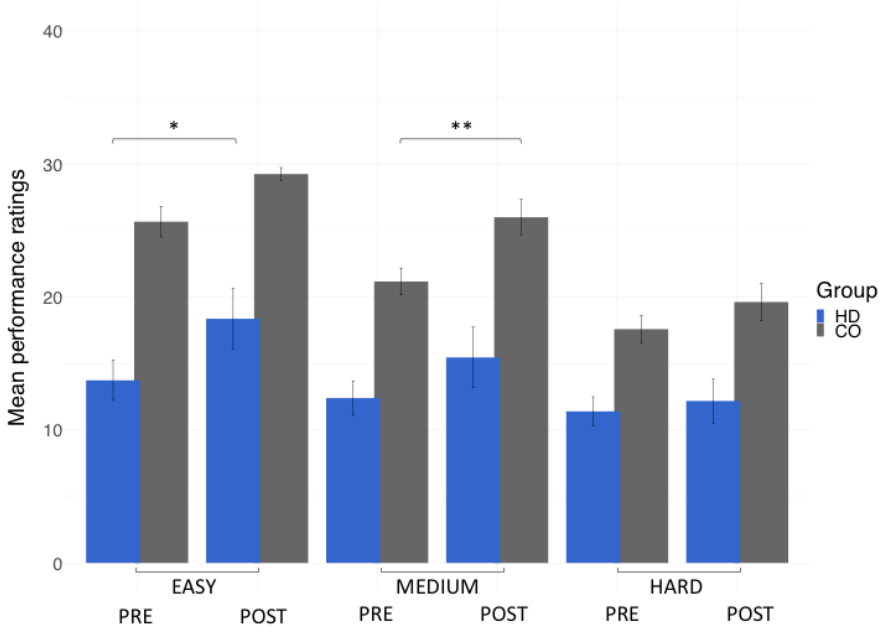

Figure 4. Mean ratings for drumming performance *according to the Trinity College London marking criteria for percussion (2016) as a function of group and time point. Patients improved their drumming performance significantly for the easy test pattern and controls for the medium difficult test pattern. * p < 0.05, ** p < 0.01, bootstrapping based on 1000 sample*

Assessment of group differences in the effect of training on cognitive performance

Three components that accounted for 79% of the variance of performance changes in the cognitive benchmark tests were extracted. The first component loaded highly on performance changes in the dual task (total number of boxes identified under dual task condition), the Stroop task (Stroop interference score), and the trails making task (Trail test switching); because all of these variables measure executive functions including focused attention and distractor suppression, the first component was labelled “executive” component. The second component loaded on variables reflecting

582 the ability to correctly recall digits sequences (i.e. number of correct digits recalled
583 under single task condition, number of correct digits recalled under dual task condition)
584 and was therefore called “working memory capacity” component. Finally, the third
585 extracted component loaded highly on verbal and category fluency, and was therefore
586 named “fluency” component (Table 4).

587 We tested whether the two groups differed in change in cognition, by running
588 permutation analyses on the individual scores for the three extracted components. The
589 HD group differed significantly from the healthy control group in the executive
590 component, t = -1.03, p = 0.008 , FDR-corrected p = 0.024. The HD group was
591 associated with positive change, whereas the control group was associated with
592 negative change in this component. However, no significant group differences were
593 detected in the other two components [Working Memory capacity: t = -0.22, p = 0.3296
594 , FDR-corrected p = 0.3296; Fluency: t = -0.39, p = 0.242 FDR corrected p = 0.3296.
595
596

597 **Training effects on WM microstructure**

598 Table 4 reports a summary of the permutation analyses of training associated
599 changes in FA, RD, Fr and MPF, across the different tracts.

600 <u>Training-associated group differences in FA</u>

601 Permutation analyses of FA changes across the different tracts revealed no
602 significant differences between HD and control groups [CCI: t = 1.22, p = 0.91 (FDR-
603 corrected); CCII: t = 2.65, p = 0.91 (FDR-corrected); CCIII: t = 0.325, p = 0.13 (FDR-
604 corrected); right SMA-Putamen: t = -9.54, p = 0.10 (FDR-corrected); left SMA-
605 Putamen: t = 5.16, p = 0.77 (FDR-corrected).

606 ***Table 4.*** *Rotated Component Loadings on Change in the Cognitive Benchmark Tests.*
607 *Significant loadings (>0.5) are highlighted in bold.*

% Change	Executive	Working memory capacity	Fluency
Total box (dual)	**0.864**	0.022	0.419
Stroop interference score	**0.811**	-0.270	-0.267
Trail test switching	**-0.731**	-0.470	0.162
Correct digits under single task condition	0.201	**0.904**	0.129
Correct digits under dual task condition	-0.193	**0.855**	-0.018
Category fluency	-0.070	-0.138	**0.817**
Verbal fluency	-0.026	-0.232	**-0.799**

608

609

610

611 Training-associated group differences in RD

612 There were no significant differences in RD changes following training
613 between HD patients and controls [CCI: t = -0.48, p = 0.45 (FDR-corrected); CCII: t =
614 -1.29, p = 0.45 (FDM-corrected); CCIII: t = -1.04, p = 0.45 (FDR-corrected); right SMA-
615 Putamen, t = 4.01 , p = 0.81 (FDR-corrected); left SMA-Putamen, t = -3.68, p = 0.39
616 (FDR-corrected).

617 Training-associated group differences in Fr

618 Permutation analyses of Fr changes across the different tracts revealed no
619 significant differences between HD and control groups [CCI: t = 3.39, p = 0.82 (FDR-

corrected; CCII: t = -0.17, p = 0.82 FDR-corrected; CCIII: t = 3.08, p = 0.82 (FDR-corrected); right SMA-Putamen: t = -5.24, p = 0.82 (FDR-corrected); left SMA-Putamen: t = 1.05, p = 0.82 (FDR-corrected)].

Training-associated group differences in MPF

PCA of change scores in MPF revealed one single component explaining 70.2% of the variance. This component presented high loadings from all the tracts investigated. A significant group difference was present for the MPF component, indicating that HD patients presented higher changes in MPF in response to training, as compared to controls [t(14) = -1.743, n = 17, p = 0.03].

Finally, we found that the mean difference in MPF change scores was significantly different between the two groups for CCII [t(14) = -20.72, p=0.04], CCIII [t(14) = -25.87, p=0.04], and the right SMA-putamen pathway [t(14) = -25.48, p=0.04] after FDR correction, therefore indicating that there was a differential effect of training between the two groups on MPF within these tracts (Figure 5).

Investigation of the relationship between training-associated changes in MRI measures and changes in drumming and cognitive performance.

We assessed whether changes in microstructure were associated with changes in drumming performance by assessing the correlation between the 'MPF' component scores and percentage changes in drumming performance. These, however, did not correlate with changes in MPF (PC1: rs = -0.14, p > 0.05).

Furthermore, to ascertain whether changes in microstructure were related to changes in cognitive performance, correlation coefficients were calculated between the 'Executive' and the 'MPF' component scores. No correlation was observed between these component scores (rho = .348, p = .171).

Investigation of baseline differences in MPF

We found a statistically significant, right-lateralised, reduction in baseline MPF in the HD group when compared to controls, in the midbody of the CC (t = 3.13, p = .05, FWE corrected). Figure 6 shows the areas that displayed a reduction of MPF in HD patients, in blue.

Discussion

Based on evidence that myelin impairment underpins WM damage in HD (Bartzokis et al., 2007), and the suggestion that myelin plasticity underlies the learning of new motor skills (Lakhani et al., 2016; Scholz et al, 2009), the present study explored whether two months of drumming training would result in changes in WM microstructure in early HD patients. Specifically, we expected to detect myelin plasticity, as indicated by changes in MPF. Further, based on evidence from studies reporting greater training-associated changes in structural MRI metrics in brain injured patients than healthy subjects (Caeyenberghs et al., 2018), we hypothesised that these changes would be present to a higher degree in HD patients than in healthy subjects.

Table 4. *Summary statistics for the permutation analysis of training effects on FA, RD, Fr and MPF, across the investigated tracts.*

MMPF	**p**	**t**	**FDR corrected p**
CCI	0.080	-12.06	0.10
CCII	0.029	-20.72	**0.04**
CCIII	0.019	-25.87	**0.04**
Left SMA-Putamen	0.380	-4.34	0.38
Right SMA-Putamen	0.018	-25.48	**0.04**
RD	**p**	**t**	**FDR corrected p**
CCI	0.358	-0.48	0.44
CCII	0.215	-1.29	0.44
CCIII	0.302	-1.04	0.44
Left SMA-Putamen	0.079	-3.68	0.39
Right SMA-Putamen	0.802	4.01	0.80
FA	**p**	**t**	**FDR corrected p**
CCI	0.909	1.22	0.91
CCII	0.910	2.65	0.91
CCIII	0.480	-0.13	0.91
Left SMA-Putamen	0.772	5.16	0.91
Right SMA-Putamen	0.023	-9.54	0.11
Fr	**p**	**t**	**FDR corrected p**
CCI	0.810	0.03	0.81
CCII	0.496	-0.001	0.81
CCIII	0.817	0.03	0.81
Left SMA-Putamen	0.582	0.01	0.81
Right SMA-Putamen	0.199	-0.05	0.81

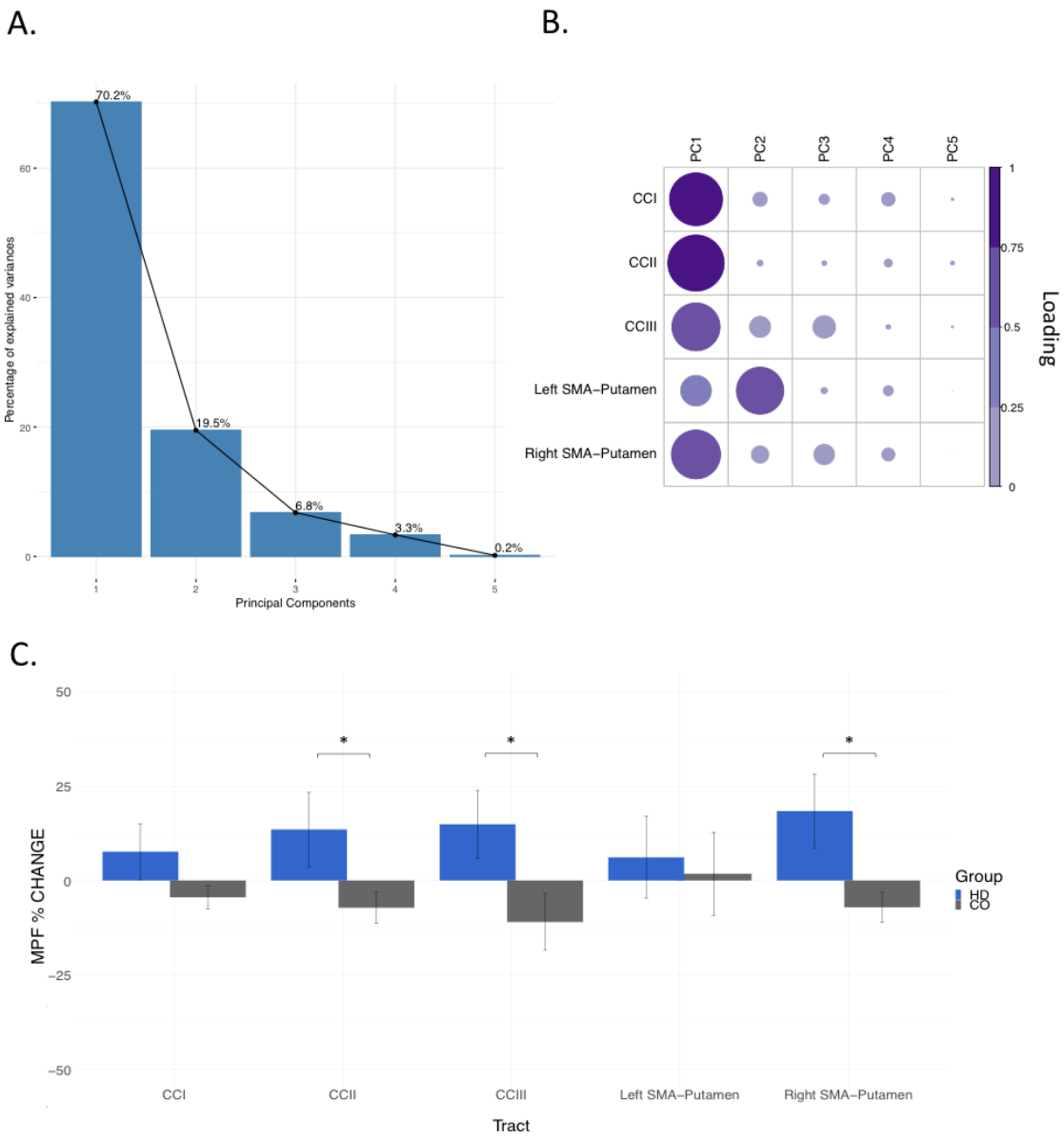

669

670 ***Figure 5. MPF changes scores****: PCA scree plot (A); correlation plot summarising*
671 *how each variable is accounted for in every principal component - colour intensity and*
672 *the size of the circles are proportional to the loading (B); Bar graph of the percentage*
673 *change in MPF across the inspected tracts; Error bars represent the standard error;*
674 *training was associated with a significantly greater change in MPF in CCII, CCIII, and*
675 *right SMA-Putamen; * (p<0.05), results corrected for multiple comparisons with FDR*
676 *(C).*

677

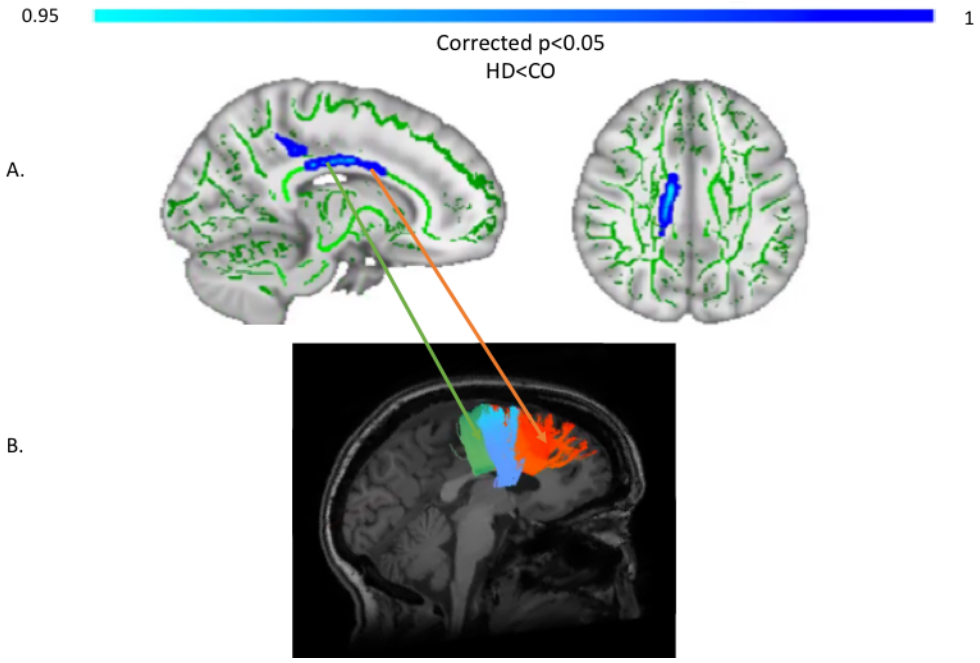

Figure 6. TBSS analysis of baseline MPF values (A)*. Light blue areas show a significant reduction of MPF in patients with HD compared to controls (p < 0.05, FWE corrected). The midbody of the CC was mostly found to be affected, which carries connections to the premotor, supplementary motor and motor areas of the brain.* ***Tracts showing significantly greater MPF changes in HD patients post-training as compared to controls (B).*** *Areas showing significant MPF reductions at baseline overlap with tracts showing significant changes post-training (i.e. CCII and CCIII).*

First, we demonstrated a behavioural effect of the drumming training by showing that patients improved their drumming performance significantly for the easy test pattern and controls for the medium test pattern. This result suggests that the training was successful in improving patients' drumming abilities.

With regards to the white matter microstructural measurements, we did not detect any group differences in training-associated changes in the diffusion based indices of FA, RD and Fr. DT-MRI metrics are influenced by the underlying fibre

696 architecture (De Santis et al., 2014). For example, in two voxels with identical axonal
697 density and myelin content, these metrics may diverge, if one of the voxels lies in a
698 region with one predominant fibre orientation, while the other lies in a region
699 presenting several crossing fibres. Though Fr from the CHARMED model enables
700 improved angular resolution as compared to DTI, this does not account for the
701 contribution of water trapped in oligodendrocyte cells or other subcellular structures
702 (Szafer, Zhong, & Gore, 1995). However, a number of human and animal studies have
703 shown oligodendrocyte changes across the lifespan in HD (Ernst et al., 2014; Gómez-
704 Tortosa et al., 2001; Jin et al., 2015; Myers et al., 1991). Therefore, while modelling
705 one (DTI) or two (CHARMED) diffusion compartments might be appropriate when
706 investigating healthy WM or other patient populations, accounting for changes in other
707 compartments of WM microstructure, such as myelin, when assessing HD patients,
708 might enable greater sensitivity to WM microstructural changes. Additionally, a study
709 investigating which metrics account for the largest inter-subject variability and
710 reporting the minimal sample sizes needed to detect an effect in diffusion measures
711 (De Santis et al., 2014), revealed that, amongst the microstructural parameters
712 investigated, FA and Fr required the largest sample size. It is therefore plausible that,
713 in the current study, we did not have enough power to detect a training-associated
714 change in these measures.

715 Through PCA of changes in MPF, we identified a single component explaining
716 most of the variability in the data which had high loadings on all the tracts investigated.
717 Moreover, we observed a significant group difference in training-associated changes
718 in the MPF component. Specifically, HD patients showed significantly increases in
719 MPF relative to controls. Furthermore, through post-hoc investigations, we detected a

720 significant difference in MPF in training-associated changes within the CCII, CCIII and
721 the right SMA-putamen pathway between patients and controls.

722 Interestingly, TBSS analysis of baseline differences in MPF suggested that
723 those areas showing significant MPF reductions at baseline were partly overlapping
724 with the tracts that showed significant changes post-training (i.e. CCII and CCIII).
725 These areas of the CC carry connections to the premotor, supplementary motor and
726 motor areas of the brain.

727 MPF can also be affected by inflammation (Henkelman, Stanisz, & Graham,
728 2001) and in manifest HD it is likely that inflammation goes hand in hand with myelin
729 breakdown (Rocha et al., 2016). However, a recent CSF biomarker study found no
730 evidence of neuro-inflammation in early-manifest HD (Vinther-Jensen et al., 2016).
731 Therefore, though preliminary, our findings suggest that two months of drumming and
732 rhythm exercises may result in myelin remodelling in patients with early HD. This, in
733 turn, suggests that tailored behavioural stimulation might be further investigated as a
734 therapeutic aiming to delay disease progression.

735 In the present study, healthy controls did not show training-associated MPF
736 changes, albeit a trend was present for negative changes. This pattern is opposite to
737 the one observed in the patients' group. In the central nervous system, axon
738 myelination has several goals, including reduction of conduction delays and lowering
739 energy costs. This idea of 'system optimization' (Chomiak & Hu, 2009) encompasses
740 several cellular mechanisms such as de novo myelination, myelin repair, adjustment
741 in conduction velocity, changes in myelin thickness (Kaller et al., 2017). These
742 dynamic changes in myelination identify a process by which an optimal status of the
743 myelinated infrastructure is identified. This, in turn, is linked to the idea of system

efficiency, whereby changes in myelin content might be dependent on where the starting point is, compared to an optimal level of myelination (Rushton, 1951). Therefore, ideal network function might not be achieved only by maximising the speed of axon conduction through increased myelination; cellular mechanisms ensuring appropriate conduction delays, as well as conduction velocity, will be equally important. Hence, it is plausible that the observed pattern of training-associated myelin remodelling may be different in healthy subjects as compared to HD patients. This is the case because HD is associated with myelin damage (Bartzokis et al., 2007), as shown by our TBSS results of reduced baseline MPF in HD patients. Furthermore, previous studies have reported that training-associated percentage changes in MRI measures tend to be higher in studies of traumatic brain injury than those shown by studies of healthy subjects (Caeyenberghs et al., 2018).

Unfortunately, analyses in the present study cannot truly disentangle the impact of prior WM microstructural differences on microstructural plasticity during learning. Notably, the behavioural effect of drumming training and cognition differed between patients and controls. Patients improved in the easy drumming test pattern, and control improved in the medium test pattern. Furthermore, patients showed increases in the executive function components whilst control participants did not improve their cognition. Therefore, different patterns of microstructural changes might not only be due to WM microstructural differences between patients and controls prior to learning, but also to a different behavioral effect of the task between HD subjects and controls. For instance, control participants performed close to ceiling in the easy test pattern, and as the training was tailored to patients' needs, some of the earlier practice sessions may not have optimally challenged them. A more taxing training for patients than controls may also explain why improvements in executive functions and apparent

myelin were only observed for the patients but not for the controls.

A critical question relevant to all training studies concerns the functional significance of any observed neural changes. In the present study, we expected microstructural changes to be related to changes in motor and cognitive functions, as assessed by drumming and cognitive tests performance (Metzler-Baddeley et al., 2014). However, we did not detect a significant relationship between changes in MRI measures and changes in drumming proficiency or performance in cognitive tests.

Other studies have failed to find a relationship between difference scores in structural MRI metrics and behavioural or clinical changes (Nordvik et al., 2012). We suggest that this might have been due to non-specific training-related neural responses. Specifically, while the training exercise might have triggered changes in brain structure, training-induced changes may not necessarily co-vary with improvements in performance. Alternatively, it might be that our study was not powered enough to detect brain-function correlations . We computed the sample size ($\alpha = 0.05$; 80% power) required to successfully detect a correlation using the GPower 3 software and found that minimum of 64 people would have to be examined to reach a medium effect size. Therefore, our results need replication in larger samples. In addition, lack of correlation between structural and functional changes after training has been reported by a number of training studies (including well-powered studies) and may suggest that these processes follow different time courses and may occur in different brain regions (Valkanova, Eguia Rodriguez, & Ebmeier, 2014).

It is important to note that our study did not include a non-intervention patient control group. Unfortunately, it was not feasible within the time period of this study to recruit a sufficiently large number of well-matched patient controls. Therefore, we cannot disentangle the effects of the training on WM microstructure from HD-

associated pathological changes. However, given that HD is a progressive neurodegenerative disease associated with demyelination (Bartzokis et al., 2007), it is very unlikely that increases in MPF observed in the patient group were due to the disease itself.

Finally, while the majority of training studies assess brain structural changes between baseline and post-training (Caeyenberghs et al., 2018), we suggest that acquiring intermittent scans during the training period could have helped to better capture and understand changes in WM microstructure observed in this study. Accordingly, future studies and more advanced statistical analyses, might be able to give greater insights into the complex nonlinear relationships between structural changes and behaviour (Thomas & Baker, 2013).

To conclude, we have demonstrated that two months of drumming and rhythm exercises result in an increase in a proxy MRI measure of myelin in patients with early HD relative to healthy controls. Whilst the current results require replication in a larger patient group with an appropriately matched patient control group, they suggest that behavioural stimulation may result in neural benefits in early HD that could be exploited for future therapeutics aiming to delay disease progression.

References

Assaf, Y., & Basser, P. J. (2005). Composite hindered and restricted model of diffusion (CHARMED) MR imaging of the human brain. *NeuroImage*, *27*(1), 48–58. https://doi.org/10.1016/j.neuroimage.2005.03.042

Aylward, E. H., Nopoulos, P. C., Ross, C. A., Langbehn, D. R., Pierson, R. K., Mills, J. A., … PREDICT-HD Investigators and Coordinators of Huntington Study Group. (2011). Longitudinal change in regional brain volumes in prodromal Huntington disease. *Journal of Neurology, Neurosurgery, and Psychiatry*, *82*(4), 405–410. https://doi.org/10.1136/jnnp.2010.208264

Baddeley, A. (1996). *Exploring the Central Executive*. 24.

Baldo, J. V., Shimamura, A. P., Delis, D. C., Kramer, J., & Kaplan, E. (2001). Verbal and design fluency in patients with frontal lobe lesions. *Journal of the International Neuropsychological Society*, *7*(5), 586–596. https://doi.org/10.1017/S1355617701755063

Barazany, D., Basser, P. J., & Assaf, Y. (2009). In vivo measurement of axon diameter distribution in the corpus callosum of rat brain. *Brain*, *132*(5), 1210–1220. https://doi.org/10.1093/brain/awp042

Bardile, C. F., Garcia-Miralles, M., Caron, N., Langley, S., Teo, R. T. Y., Petretto, E., … Pouladi, M. A. (2018). A43 Intrinsic mutant HTT-mediated defects in oligodendroglia cells contribute to myelin deficits and behavioural abnormalities in huntington disease. *J Neurol Neurosurg Psychiatry*, *89*(Suppl 1), A15–A16. https://doi.org/10.1136/jnnp-2018-EHDN.41

Bartzokis, G., Lu, P. H., Tishler, T. A., Fong, S. M., Oluwadara, B., Finn, J. P., … Perlman, S. (2007). Myelin breakdown and iron changes in Huntington's disease: Pathogenesis and treatment implications. *Neurochemical Research*, *32*(10), 1655–1664. https://doi.org/10.1007/s11064-007-9352-7

Beglinger, L. J., Langbehn, D. R., Duff, K., Stierman, L., Black, D. W., Nehl, C., … Huntington Study Group Investigators. (2007). Probability of obsessive and compulsive symptoms in Huntington's disease. *Biological Psychiatry*, *61*(3), 415–418. https://doi.org/10.1016/j.biopsych.2006.04.034

Ben-Amitay, S., Jones, D. K., & Assaf, Y. (2012). Motion correction and registration of high b-value diffusion weighted images. *Magnetic Resonance in Medicine*, *67*(6), 1694–1702. https://doi.org/10.1002/mrm.23186

Benjamini, Y., & Hochberg, Y. (1995). Controlling the False Discovery Rate: A Practical and Powerful Approach to Multiple Testing. *Journal of the Royal Statistical Society. Series B (Methodological)*, *57*(1), 289–300. Retrieved from JSTOR.

Bourbon-Teles, J., Bells, S., Jones, D. K., Coulthard, E., Rosser, A., & Metzler-Baddeley, C. (2017). Myelin breakdown in human Huntington's disease: Multi-modal evidence from diffusion MRI and quantitative magnetization transfer. *Neuroscience*. https://doi.org/10.1016/j.neuroscience.2017.05.042

Caeyenberghs, K., Clemente, A., Imms, P., Egan, G., Hocking, D. R., Leemans, A., … Wilson, P. H. (2018). Evidence for Training-Dependent Structural Neuroplasticity in Brain-Injured Patients: A Critical Review. *Neurorehabilitation and Neural Repair*, *32*(2), 99–114. https://doi.org/10.1177/1545968317753076

Cattell, R. B. (1966). The Scree Test For The Number Of Factors. *Multivariate Behavioral Research*, *1*(2), 245–276. https://doi.org/10.1207/s15327906mbr0102_10

Cercignani, M., & Alexander, D. C. (2006). Optimal acquisition schemes for in vivo quantitative magnetization transfer MRI. *Magnetic Resonance in Medicine*, *56*(4), 803–810. https://doi.org/10.1002/mrm.21003

Chomiak, T., & Hu, B. (2009). What Is the Optimal Value of the g-Ratio for Myelinated Fibers in the Rat CNS? A Theoretical Approach. *PLOS ONE*, *4*(11), e7754. https://doi.org/10.1371/journal.pone.0007754

Ciarmiello, A., Cannella, M., Lastoria, S., Simonelli, M., Frati, L., Rubinsztein, D. C., & Squitieri, F. (2006). Brain white-matter volume loss and glucose hypometabolism precede the clinical symptoms of Huntington's disease. *Journal of Nuclear Medicine: Official Publication, Society of Nuclear Medicine*, *47*(2), 215–222.

Costa, R. M., Cohen, D., & Nicolelis, M. A. L. (2004). Differential corticostriatal plasticity during fast and slow motor skill learning in mice. *Current Biology: CB*, *14*(13), 1124–1134. https://doi.org/10.1016/j.cub.2004.06.053

De Santis, S., Drakesmith, M., Bells, S., Assaf, Y., & Jones, D. K. (2014). Why diffusion tensor MRI does well only some of the time: Variance and covariance of white matter tissue microstructure attributes in the living human brain. *Neuroimage*, *89*(100), 35–44. https://doi.org/10.1016/j.neuroimage.2013.12.003

Dell'acqua, F., Scifo, P., Rizzo, G., Catani, M., Simmons, A., Scotti, G., & Fazio, F. (2010). A modified damped Richardson-Lucy algorithm to reduce isotropic background effects in spherical deconvolution. *NeuroImage*, *49*(2), 1446–1458. https://doi.org/10.1016/j.neuroimage.2009.09.033

Diana Rosas, H., Lee, S. Y., Bender, A., Zaleta, A. K., Vange, M., Yu, P., … Hersch, S. M. (2010). Altered White Matter Microstructure in the Corpus Callosum in Huntington's Disease: Implications for cortical "disconnection." *NeuroImage*, *49*(4), 2995–3004. https://doi.org/10.1016/j.neuroimage.2009.10.015

Dumas, E. M., van den Bogaard, S. J. A., Ruber, M. E., Reilman, R. R., Stout, J. C., Craufurd, D., … Roos, R. A. C. (2012). Early changes in white matter pathways of the sensorimotor cortex in premanifest Huntington's disease. *Human Brain Mapping*, *33*(1), 203–212. https://doi.org/10.1002/hbm.21205

Ernst, A., Alkass, K., Bernard, S., Salehpour, M., Perl, S., Tisdale, J., … Frisén, J. (2014). Neurogenesis in the Striatum of the Adult Human Brain. *Cell*, *156*(5), 1072–1083. https://doi.org/10.1016/j.cell.2014.01.044

Giacosa, C., Karpati, F. J., Foster, N. E. V., Penhune, V. B., & Hyde, K. L. (2016). Dance and music training have different effects on white matter diffusivity in sensorimotor pathways. *NeuroImage*, *135*, 273–286. https://doi.org/10.1016/j.neuroimage.2016.04.048

Gómez-Tortosa, E., MacDonald, M. E., Friend, J. C., Taylor, S. A., Weiler, L. J., Cupples, L. A., … Myers, R. H. (2001). Quantitative neuropathological changes in presymptomatic Huntington's disease. *Annals of Neurology*, *49*(1), 29–34.

Gregory, S., Crawford, H., Seunarine, K., Leavitt, B., Durr, A., Roos, R. A. C., … Orth, M. (2018). Natural biological variation of white matter microstructure is accentuated in Huntington's disease. *Human Brain Mapping*, *39*(9), 3516–3527. https://doi.org/10.1002/hbm.24191

Grydeland, H., Walhovd, K. B., Tamnes, C. K., Westlye, L. T., & Fjell, A. M. (2013). Intracortical myelin links with performance variability across the human lifespan: Results from T1- and T2-weighted MRI myelin mapping and diffusion tensor imaging. *The Journal of Neuroscience: The Official Journal of the Society for Neuroscience*, *33*(47), 18618–18630. https://doi.org/10.1523/JNEUROSCI.2811-13.2013

Henkelman, R. M., Stanisz, G. J., & Graham, S. J. (n.d.). Magnetization transfer in MRI: A review. *NMR in Biomedicine*, *14*(2), 57–64. https://doi.org/10.1002/nbm.683

Hofer, S., & Frahm, J. (2006). Topography of the human corpus callosum revisited—Comprehensive fiber tractography using diffusion tensor magnetic resonance imaging. *NeuroImage*, *32*(3), 989–994. https://doi.org/10.1016/j.neuroimage.2006.05.044

Hofstetter, S., Tavor, I., Moryosef, S. T., & Assaf, Y. (2013). Short-Term Learning Induces White Matter Plasticity in the Fornix. *Journal of Neuroscience*, *33*(31), 12844–12850. https://doi.org/10.1523/JNEUROSCI.4520-12.2013

Huang, B., Wei, W., Wang, G., Gaertig, M. A., Feng, Y., Wang, W., … Li, S. (2015). Mutant huntingtin downregulates myelin regulatory factor-mediated myelin

gene expression and affects mature oligodendrocytes. *Neuron*, *85*(6), 1212–1226. https://doi.org/10.1016/j.neuron.2015.02.026

Irfanoglu, M. O., Walker, L., Sarlls, J., Marenco, S., & Pierpaoli, C. (2012). Effects of image distortions originating from susceptibility variations and concomitant fields on diffusion MRI tractography results. *NeuroImage*, *61*(1), 275–288. https://doi.org/10.1016/j.neuroimage.2012.02.054

Jeurissen, B., Leemans, A., Jones, D. K., Tournier, J.-D., & Sijbers, J. (2011). Probabilistic fiber tracking using the residual bootstrap with constrained spherical deconvolution. *Human Brain Mapping*, *32*(3), 461–479. https://doi.org/10.1002/hbm.21032

Jin, J., Peng, Q., Hou, Z., Jiang, M., Wang, X., Langseth, A. J., … Duan, W. (2015). Early white matter abnormalities, progressive brain pathology and motor deficits in a novel knock-in mouse model of Huntington's disease. *Human Molecular Genetics*, *24*(9), 2508–2527. https://doi.org/10.1093/hmg/ddv016

Kaller, M. S., Lazari, A., Blanco-Duque, C., Sampaio-Baptista, C., & Johansen-Berg, H. (2017). Myelin plasticity and behaviour—Connecting the dots. *Current Opinion in Neurobiology*, *47*, 86–92. https://doi.org/10.1016/j.conb.2017.09.014

Klein, S., Staring, M., Murphy, K., Viergever, M. A., & Pluim, J. P. W. (2010). elastix: A toolbox for intensity-based medical image registration. *IEEE Transactions on Medical Imaging*, *29*(1), 196–205. https://doi.org/10.1109/TMI.2009.2035616

Lakhani, B., Borich, M. R., Jackson, J. N., Wadden, K. P., Peters, S., Villamayor, A., … Boyd, L. A. (2016). Motor Skill Acquisition Promotes Human Brain Myelin Plasticity [Research article]. https://doi.org/10.1155/2016/7526135

Leemans, A, Jeurissen, B., Sijbers, J., & Jones, D. K. (n.d.). *ExploreDTI: a graphical toolbox for processing, analyzing, and visualizing diffusion MR data*. 1.

Leemans, Alexander, & Jones, D. K. (2009). The B-matrix must be rotated when correcting for subject motion in DTI data. *Magnetic Resonance in Medicine*, *61*(6), 1336–1349. https://doi.org/10.1002/mrm.21890

Leh, S. E., Ptito, A., Chakravarty, M. M., & Strafella, A. P. (2007). Fronto-striatal connections in the human brain: A probabilistic diffusion tractography study. *Neuroscience Letters*, *419*(2), 113–118. https://doi.org/10.1016/j.neulet.2007.04.049

Levesque, I. R., Giacomini, P. S., Narayanan, S., Ribeiro, L. T., Sled, J. G., Arnold, D. L., & Pike, G. B. (2010). Quantitative magnetization transfer and myelin water imaging of the evolution of acute multiple sclerosis lesions. *Magnetic Resonance in Medicine*, *63*(3), 633–640. https://doi.org/10.1002/mrm.22244

Lövdén, M., Bodammer, N. C., Kühn, S., Kaufmann, J., Schütze, H., Tempelmann, C., … Lindenberger, U. (2010). Experience-dependent plasticity of white-matter microstructure extends into old age. *Neuropsychologia*, *48*(13), 3878–3883. https://doi.org/10.1016/j.neuropsychologia.2010.08.026

Martenson, R. E. (1992). *Myelin*. CRC Press.

McKenzie, I. A., Ohayon, D., Li, H., de Faria, J. P., Emery, B., Tohyama, K., & Richardson, W. D. (2014). Motor skill learning requires active central myelination. *Science (New York, N.Y.)*, *346*(6207), 318–322. https://doi.org/10.1126/science.1254960

Metzler-Baddeley, C., Cantera, J., Coulthard, E., Rosser, A., Jones, D. K., & Baddeley, R. J. (2014). Improved Executive Function and Callosal White Matter Microstructure after Rhythm Exercise in Huntington's Disease. *Journal of Huntington's Disease*, *3*(3), 273–283. https://doi.org/10.3233/JHD-140113

Metzler-Baddeley, C., O'Sullivan, M. J., Bells, S., Pasternak, O., & Jones, D. K. (2012). How and how not to correct for CSF-contamination in diffusion MRI. *NeuroImage*, *59*(2), 1394–1403. https://doi.org/10.1016/j.neuroimage.2011.08.043

Myers, R. H., Vonsattel, J. P., Paskevich, P. A., Kiely, D. K., Stevens, T. J., Cupples, L. A., … Bird, E. D. (1991). Decreased Neuronal and Increased Oligodendroglial Densities in Huntington's Disease Caudate Nucleus. *Journal of Neuropathology & Experimental Neurology*, *50*(6), 729–742. https://doi.org/10.1097/00005072-199111000-00005

Nasreddine, Z. S., Phillips, N. A., Bédirian, V., Charbonneau, S., Whitehead, V., Collin, I., … Chertkow, H. (2005). The Montreal Cognitive Assessment, MoCA: A Brief Screening Tool For Mild Cognitive Impairment. *Journal of the American Geriatrics Society*, *53*(4), 695–699. https://doi.org/10.1111/j.1532-5415.2005.53221.x

Nelson, H. (n.d.). *National Adult Reading Test (NART) test manual (Part 1*. Retrieved from https://www.academia.edu/2515150/National_Adult_Reading_Test_NART_test_manual_Part_1

Nordvik, J. E., Schanke, A.-K., Walhovd, K., Fjell, A., Grydeland, H., & Landrø, N. I. (2012). Exploring the relationship between white matter microstructure and working memory functioning following stroke: A single case study of computerized cognitive training. *Neurocase*, *18*(2), 139–151. https://doi.org/10.1080/13554794.2011.568501

Ou, X., Sun, S.-W., Liang, H.-F., Song, S.-K., & Gochberg, D. F. (2009). The MT pool size ratio and the DTI radial diffusivity may reflect the myelination in shiverer and control mice. *NMR in Biomedicine*, *22*(5), 480–487. https://doi.org/10.1002/nbm.1358

Pajevic, S., & Pierpaoli, C. (1999). Color schemes to represent the orientation of anisotropic tissues from diffusion tensor data: Application to white matter fiber tract mapping in the human brain. *Magnetic Resonance in Medicine*, *42*(3), 526–540.

Paulsen, J. S., Langbehn, D. R., Stout, J. C., Aylward, E., Ross, C. A., Nance, M., … Predict-HD Investigators and Coordinators of the Huntington Study Group. (2008). Detection of Huntington's disease decades before diagnosis: The Predict-HD study. *Journal of Neurology, Neurosurgery, and Psychiatry*, *79*(8), 874–880. https://doi.org/10.1136/jnnp.2007.128728

Penke, L., Maniega, S. M., Murray, C., Gow, A. J., Hernández, M. C. V., Clayden, J. D., … Deary, I. J. (2010). A General Factor of Brain White Matter Integrity Predicts Information Processing Speed in Healthy Older People. *Journal of Neuroscience*, *30*(22), 7569–7574. https://doi.org/10.1523/JNEUROSCI.1553-10.2010

Phillips, O., Sanchez-Castaneda, C., Elifani, F., Maglione, V., Pardo, A. D., Caltagirone, C., … Paola, M. D. (2013). Tractography of the Corpus Callosum in Huntington's Disease. *PLOS ONE*, *8*(9), e73280. https://doi.org/10.1371/journal.pone.0073280

Pierpaoli, C., & Basser, P. J. (1996). Toward a quantitative assessment of diffusion anisotropy. *Magnetic Resonance in Medicine*, *36*(6), 893–906.

Poudel, G. R., Stout, J. C., Domínguez D, J. F., Salmon, L., Churchyard, A., Chua, P., … Egan, G. F. (2014). White matter connectivity reflects clinical and cognitive status in Huntington's disease. *Neurobiology of Disease*, *65*, 180–187. https://doi.org/10.1016/j.nbd.2014.01.013

Preacher, K. J., & MacCallum, R. C. (2002). Exploratory Factor Analysis in Behavior Genetics Research: Factor Recovery with Small Sample Sizes. *Behavior Genetics*, *32*(2), 153–161. https://doi.org/10.1023/A:1015210025234

Reading, S. A. J., Yassa, M. A., Bakker, A., Dziorny, A. C., Gourley, L. M., Yallapragada, V., … Ross, C. A. (2005). Regional white matter change in pre-symptomatic Huntington's disease: A diffusion tensor imaging study. *Psychiatry Research*, *140*(1), 55–62. https://doi.org/10.1016/j.pscychresns.2005.05.011

1041 Rocha, N. P., Ribeiro, F. M., Furr-Stimming, E., & Teixeira, A. L. (2016).
1042 Neuroimmunology of Huntington's Disease: Revisiting Evidence from Human
1043 Studies. *Mediators of Inflammation*, *2016*.
1044 https://doi.org/10.1155/2016/8653132

1045 Rosas, H. D., Wilkens, P., Salat, D. H., Mercaldo, N. D., Vangel, M., Yendiki, A. Y., &
1046 Hersch, S. M. (2018). Complex spatial and temporally defined myelin and
1047 axonal degeneration in Huntington disease. *NeuroImage: Clinical*, *20*, 236–
1048 242. https://doi.org/10.1016/j.nicl.2018.01.029

1049 Rushton, W. A. H. (1951). A theory of the effects of fibre size in medullated nerve.
1050 *The Journal of Physiology*, *115*(1), 101–122.

1051 Sampaio-Baptista, C., Khrapitchev, A. A., Foxley, S., Schlagheck, T., Scholz, J.,
1052 Jbabdi, S., … Johansen-Berg, H. (2013). Motor Skill Learning Induces
1053 Changes in White Matter Microstructure and Myelination. *The Journal of*
1054 *Neuroscience*, *33*(50), 19499–19503.
1055 https://doi.org/10.1523/JNEUROSCI.3048-13.2013

1056 Schmierer, K., Tozer, D. J., Scaravilli, F., Altmann, D. R., Barker, G. J., Tofts, P. S.,
1057 & Miller, D. H. (2007). Quantitative Magnetization Transfer Imaging in
1058 Postmortem Multiple Sclerosis Brain. *Journal of Magnetic Resonance*
1059 *Imaging : JMRI*, *26*(1), 41–51. https://doi.org/10.1002/jmri.20984

1060 Scholz, J., Klein, M. C., Behrens, T. E. J., & Johansen-Berg, H. (2009). Training
1061 induces changes in white matter architecture. *Nature Neuroscience*, *12*(11),
1062 1370–1371. https://doi.org/10.1038/nn.2412

Serres, S., Anthony, D. C., Jiang, Y., Campbell, S. J., Broom, K. A., Khrapitchev, A., & Sibson, N. R. (2009). Comparison of MRI signatures in pattern I and II multiple sclerosis models. *NMR in Biomedicine*, *22*(10), 1014–1024. https://doi.org/10.1002/nbm.1404

Shmuelof, L., & Krakauer, J. W. (2011). Are we ready for a natural history of motor learning? *Neuron*, *72*(3), 469–476. https://doi.org/10.1016/j.neuron.2011.10.017

Simmons, D. A., Casale, M., Alcon, B., Pham, N., Narayan, N., & Lynch, G. (n.d.). Ferritin accumulation in dystrophic microglia is an early event in the development of Huntington's disease. *Glia*, *55*(10), 1074–1084. https://doi.org/10.1002/glia.20526

Sled, J. G. (2018). Modelling and interpretation of magnetization transfer imaging in the brain. *NeuroImage*, *182*, 128–135. https://doi.org/10.1016/j.neuroimage.2017.11.065

Smith, S. M., Jenkinson, M., Johansen-Berg, H., Rueckert, D., Nichols, T. E., Mackay, C. E., … Behrens, T. E. J. (2006). Tract-based spatial statistics: Voxelwise analysis of multi-subject diffusion data. *NeuroImage*, *31*(4), 1487–1505. https://doi.org/10.1016/j.neuroimage.2006.02.024

Steele, C. J., Bailey, J. A., Zatorre, R. J., & Penhune, V. B. (2013). Early musical training and white-matter plasticity in the corpus callosum: Evidence for a sensitive period. *The Journal of Neuroscience: The Official Journal of the Society for Neuroscience*, *33*(3), 1282–1290. https://doi.org/10.1523/JNEUROSCI.3578-12.2013

Szafer, A., Zhong, J., & Gore, J. C. (1995). Theoretical Model for Water Diffusion in Tissues. *Magnetic Resonance in Medicine*, *33*(5), 697–712. https://doi.org/10.1002/mrm.1910330516

Tabrizi, S. J., Langbehn, D. R., Leavitt, B. R., Roos, R. A., Durr, A., Craufurd, D., … TRACK-HD investigators. (2009). Biological and clinical manifestations of Huntington's disease in the longitudinal TRACK-HD study: Cross-sectional analysis of baseline data. *The Lancet. Neurology*, *8*(9), 791–801. https://doi.org/10.1016/S1474-4422(09)70170-X

Teo, R. T. Y., Hong, X., Yu-Taeger, L., Huang, Y., Tan, L. J., Xie, Y., … Pouladi, M. A. (2016). Structural and molecular myelination deficits occur prior to neuronal loss in the YAC128 and BACHD models of Huntington disease. *Human Molecular Genetics*, *25*(13), 2621–2632. https://doi.org/10.1093/hmg/ddw122

Testa, R., Bennett, P., & Ponsford, J. (2012). Factor analysis of nineteen executive function tests in a healthy adult population. *Archives of Clinical Neuropsychology: The Official Journal of the National Academy of Neuropsychologists*, *27*(2), 213–224. https://doi.org/10.1093/arclin/acr112

Thomas, C., & Baker, C. I. (2013). Teaching an adult brain new tricks: A critical review of evidence for training-dependent structural plasticity in humans. *NeuroImage*, *73*, 225–236. https://doi.org/10.1016/j.neuroimage.2012.03.069

Trenerry M. R., Crosson B., DeBoe J., Leber W. R.. , Stroop Neuropsychological Screening Test , 1989Odessa, FLPsychological Assessment Resources

Valkanova, V., Eguia Rodriguez, R., & Ebmeier, K. P. (2014). Mind over matter—What do we know about neuroplasticity in adults? *International*

Psychogeriatrics, *26*(6), 891–909. https://doi.org/10.1017/S1041610213002482

van Dellen, A., Blakemore, C., Deacon, R., York, D., & Hannan, A. J. (2000). Delaying the onset of Huntington's in mice. *Nature*, *404*(6779), 721–722. https://doi.org/10.1038/35008142

Vinther-Jensen, T., Simonsen, A. H., Budtz-Jørgensen, E., Hjermind, L. E., & Nielsen, J. E. (n.d.). Ubiquitin: A potential cerebrospinal fluid progression marker in Huntington's disease. *European Journal of Neurology*, *22*(10), 1378–1384. https://doi.org/10.1111/ene.12750

Vonsattel, J. P. G., & Difiglia, M. (1998). Huntington Disease. *Journal of Neuropathology & Experimental Neurology*, *57*(5), 369–384. https://doi.org/10.1097/00005072-199805000-00001

Wahl, M., Li, Y.-O., Ng, J., Lahue, S. C., Cooper, S. R., Sherr, E. H., & Mukherjee, P. (2010). Microstructural correlations of white matter tracts in the human brain. *NeuroImage*, *51*(2), 531–541. https://doi.org/10.1016/j.neuroimage.2010.02.072

Wang, N., & Yang, X. W. (2019). Huntington Disease's Glial Progenitor Cells Hit the Pause Button in the Mouse Brain. *Cell Stem Cell*, *24*(1), 3–4. https://doi.org/10.1016/j.stem.2018.12.004

Weaver, K. E., Richards, T. L., Liang, O., Laurino, M. Y., Samii, A., & Aylward, E. H. (2009). Longitudinal diffusion tensor imaging in Huntington's Disease. *Experimental Neurology*, *216*(2), 525–529. https://doi.org/10.1016/j.expneurol.2008.12.026

Wheeler-Kingshott, C. A. M., & Cercignani, M. (2009). About “axial” and “radial” diffusivities. *Magnetic Resonance in Medicine*, *61*(5), 1255–1260. https://doi.org/10.1002/mrm.21965

Winter*, J. C. F. de, Dodou*, D., & Wieringa, P. A. (2009). Exploratory Factor Analysis With Small Sample Sizes. *Multivariate Behavioral Research*, *44*(2), 147–181. https://doi.org/10.1080/00273170902794206

Yhnell, E., Lelos, M. J., Dunnett, S. B., & Brooks, S. P. (2016). Cognitive training modifies disease symptoms in a mouse model of Huntington’s disease. *Experimental Neurology*, *282*, 19–26. https://doi.org/10.1016/j.expneurol.2016.05.008

Yin, H. H., Mulcare, S. P., Hilário, M. R. F., Clouse, E., Holloway, T., Davis, M. I., … Costa, R. M. (2009). Dynamic reorganization of striatal circuits during the acquisition and consolidation of a skill. *Nature Neuroscience*, *12*(3), 333–341. https://doi.org/10.1038/nn.2261

Zatorre, R. J., Fields, R. D., & Johansen-Berg, H. (2012). Plasticity in gray and white: Neuroimaging changes in brain structure during learning. *Nature Neuroscience*, *15*(4), 528–536. https://doi.org/10.1038/nn.3045